

On the origin of asymmetric fission of actinides

Guillaume Scamps*

Center for Computational Sciences, University of Tsukuba, Tsukuba 305-8571, Japan

Cédric Simenel†

Department of Nuclear Physics, Research School of Physics and Engineering
Australian National University, Canberra, Australian Capital Territory 2601, Australia

Background: Nuclear fission of most actinides near the valley of stability is dominated by asymmetric modes with a heavy fragment charge distribution centered around $Z \approx 52 - 55$ protons. Although spherical shell effects in the ^{132}Sn are often considered as a driver for the formation of the heavy fragment, a convincing explanation for the origin of actinide asymmetric fission has been lacking so far.

Purpose: To propose an explanation based on the couplings between fission dynamics and octupole deformations in the fragments, with the octupole correlations in the ^{144}Ba region as a driver to asymmetric split.

Method: Constrained and time-dependent Hartree-Fock microscopic calculations with dynamical pairing correlations have been performed for a series of actinides to compute expectation values of proton and neutron numbers in the fission fragments, their total kinetic energy (TKE), and their octupole and quadrupole deformations.

Results: Deformed shell gaps are present at $Z = 52$ and 56 in ^{142}Xe and are particularly stable against octupole deformation. Heavy fission fragments are almost exclusively produced with $\langle Z \rangle \approx 52 - 56$ and a significant octupole deformation at scission. Fragments with $\langle Z \rangle \approx 54 - 56$ are more deformed, leading to a smaller TKE than $\langle Z \rangle \approx 52$ fragments, in good agreement with experimental observations.

Conclusions: Asymmetric fission of actinides is induced by octupole softness in the ^{144}Ba region and not by spherical shell effects in the ^{132}Sn region, except in symmetric fission of fermium isotopes in which both fragments are close to Sn.

PACS numbers: 24.75.+i, 21.60.Jz, 27.90.+b

Keywords: fission, TDHF, pairing

INTRODUCTION

Nuclear fission is a good textbook example of how quantum dynamics can differ from classical one. This is nicely illustrated by the mass distributions of the fragments formed in low-energy fission of many actinide nuclei: While classical approach predicts a symmetric fission induced by the Coulomb repulsion, experimental mass fragment distributions often exhibit strong asymmetries. Interestingly, the origin of this characteristic of low-energy fission process is still unclear.

The observation of mass asymmetric fission traces back to the discovery of fission itself by Hahn and Strassmann [1] who proved the existence of barium ($Z = 56$ protons) in uranium ($Z = 92$) samples irradiated by neutrons. The interpretation in terms of fission of the uranium nuclei by Meitner and Frisch [2] implied the formation of a lighter krypton ($Z = 36$) complementary fission fragment. This mass asymmetry of fission fragments is a general feature in the actinides and it is the subject of many current experimental programs [3–12].

A remarkable stability of the centroid of the heavy fragment mass distribution in actinide fission has been found around $A \approx 142$ nucleons [13, 14]. In fact, detailed analyses of the shape of fragment mass distributions indicate two asymmetric fission modes: the so-called Standard 1 (St1) and Standard 2 (St2) “Brosa modes” [15] centred around $A = 135$ and $A = 142$, respectively. A transition

to a symmetric fission mode is also observed for neutron deficient actinides [3].

The standard interpretation that St1 is due to the spherical shell effects in the $N = 82$ region ($N = 82$ is a so-called “magic number”, bringing additional stability due to quantum shell closures) and that St2 is due to the $N \approx 88$ deformed shell closure [16, 17] has been challenged ten years ago [18] by the experimental observation that St1 and St2 were in fact associated with constant numbers of protons centred around $\langle Z \rangle \approx 52.5$ and 55 , respectively, and that the number of neutrons had little (if any) influence.

Although one can successfully reproduce fission-fragment mass distributions by incorporating these fission modes in a statistical method [19], or even by using dynamical approaches [20–24] based on fully microscopic potential energy surfaces [25], the origin of the stability in the $Z = 52 - 55$ region remains unexplained. Several ideas have been proposed [26], such as (i) an absorption of the neck by the heavy fragment (thus St1 could be due to its proximity with the $Z = 50$ magic number), or (ii) shell-model calculations miss proton shell effects near $Z = 55$, or (iii) quantum shell effects play a different role on fission than what was expected. It should be noted, however, that in quasifission (fission of a system formed by the capture of two heavy nuclei without formation of an equilibrated compound nucleus), shell effects strongly favour the formation of fission fragments with the sph-

ical magic number $Z = 82$ protons [27, 28].

The purpose of this work is to investigate the origin of asymmetric fission in actinide atomic nuclei with a theoretical approach which is time-dependent and microscopic in order to account for both dynamical and quantum shell effects. Recent applications based on the time-dependent Hartree-Fock (TDHF) mean-field approach [29–31] and using its BCS [32–34] and Bogoliubov [35] extensions to account for superfluidity have been performed to study fission dynamics during the descent of the potential towards scission, with initial configurations outside the fission barrier and before the preformation of the fragments [29, 32, 36]. In the present work, we use a 3-dimensional TDHF+BCS code [32, 37] with the SLy4d parametrization [38] of the Skyrme energy density functional [39]. Following the same technique as in Ref. [32], the initial configurations for the time-dependent calculations are generated by constrained Hartree-Fock+BCS (CHF+BCS) calculations [40] with a combination of quadrupole and octupole constraints. The other multipole moments are not constrained. Once in the chosen fission valley, the octupole constraint is released to allow the system to find a local minimum of energy for a given quadrupole deformation [32]. Various initial configurations produced with different deformations are considered to investigate the influence of the initial condition on the final properties of the fragments. Contrary to earlier concerns [33, 35], this procedure allows the system to fission starting from compact configurations just after the fission saddle point and without additional boosts [34]. More details of the calculations can be found in the supplemental material [41].

Figure 1 shows isodensities obtained from a dynamical evolution of ^{240}Pu starting from a configuration with quadrupole moment $Q_{20} = 45.4$ b. In this example, scission occurs after ~ 20 zs. Although this time can vary strongly with the initial configuration (up to ~ 90 zs) [41], its order of magnitude is comparable to what is found with a Bogoliubov treatment of pairing correlations [35], indicating that the BCS approximation allows for similar complex exploration of paths to fission. Similar calculations have been performed with different initial quadrupole moments and for ^{230}Th , $^{234,236}\text{U}$, ^{246}Cm and ^{250}Cf actinides (see [41]). As shown in Fig. 2, almost all heavy fragments are formed with $Z = 52 - 55$ protons, in excellent agreement with experimental observation [13]. Note that the fragments are slightly more neutron-rich (typically one additional neutron) than what would be expected if they had the neutron-to-proton ratio of the fissioning nucleus.

In order to understand the mechanisms responsible for the production of these fragments, we now investigate the preformation of the fission fragments. The latter can be identified from their shell structure using the Fermion localization function [42] which has been recently applied to nuclear systems [43] including in fission [36] and reac-

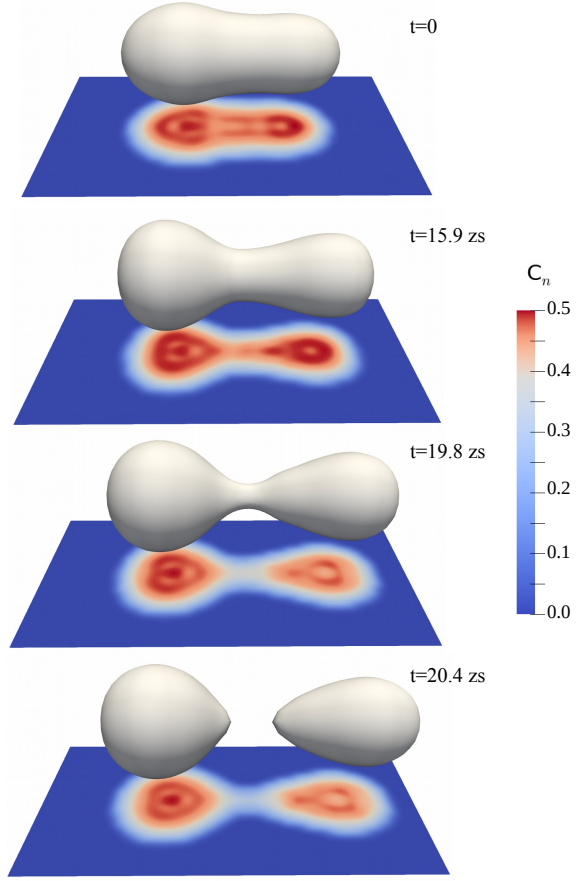


FIG. 1. Isodensity at half the saturation density $\rho_0/2 = 0.08 \text{ fm}^{-3}$ (grey surface) of ^{240}Pu fissioning system at four different times. The heavy fragment has about 54 protons and 85 neutrons. The localisation function C_n of the neutrons in the central horizontal plane is shown in the lower projections.

tion studies [44]. The stability of the neutron localization function shown in Fig. 1 (see [41] for details) in the later stages of fission indicates that the shell structures signing the preformation of the fragments are present well before scission (at about 4 zs before scission in this example).

Interestingly, the isodensity and the localization function also indicate a quadrupole as well as a strong octupole deformation of the preformed fragments. The octupole deformation of the fragments, often neglected [45], has been indeed recently shown to play an important role at scission [46]. It is well known that couplings between relative motion and low-lying collective octupole excitations play an important role in the capture process occurring in the early stage of heavy-ion fusion by lowering the so-called fusion barrier [47–51]. The capture mechanism can naively be seen as the “reverse” process to scission

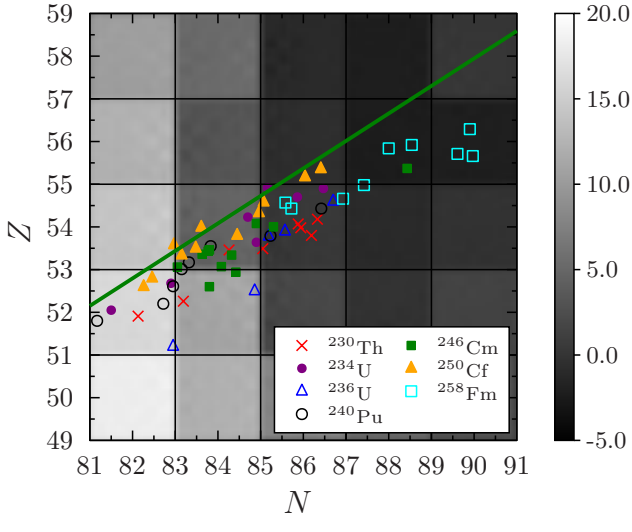


FIG. 2. Expectation values of the number of protons and neutrons in the heavy fragments for various asymmetric fissions. The solid line shows the expected positions of fragments with the N/Z neutron-to-proton number ratio values of ^{240}Pu . The background colors quantify the octupole stiffness in the nuclei as predicted by CHF+BCS calculations (see text and supplemental material [41]). Negative values indicate nuclei likely to exhibit octupole deformations in their ground-state.

occurring at the late stage of nuclear fission. Therefore, it is not surprising that similar couplings to octupole shapes impact the fission dynamics, favouring the formation of fission fragments which exhibit an octupole softness. Of course, a similar role is played by the quadrupole couplings (see for instance the strong quadrupole deformation of the light fragment in Fig. 1). However, as a majority of nuclei exhibit a quadrupole deformation in their ground nuclei, this cannot be the reason for the specific location of the St1 and St2 modes.

The situation is different for octupole correlations where only few regions of the nuclear chart have been identified as good candidates for exhibiting an octupole softness which is strong enough to induce octupole deformations in the ground-state itself [52–55]. In particular, strong octupole correlations have been recently measured in ^{144}Ba ($Z = 56$) [54], which is a possible heavy fragment in asymmetric fission of actinides. Nuclei close to ^{144}Ba in the nuclear chart could as well exhibit a particularly strong octupole softness thereby providing a possible explanation to the favoured production of these nuclei in fission. Microscopic approaches like the ones used here automatically incorporate the possibility for the nuclei to acquire octupole deformations induced by their underlying quantum shell structure. This is illustrated in Fig. 3 showing the potential energy surface of ^{142}Xe , another possible fission fragment, and predicting a quadrupole

and octupole deformed mean-field ground-state for this nucleus.

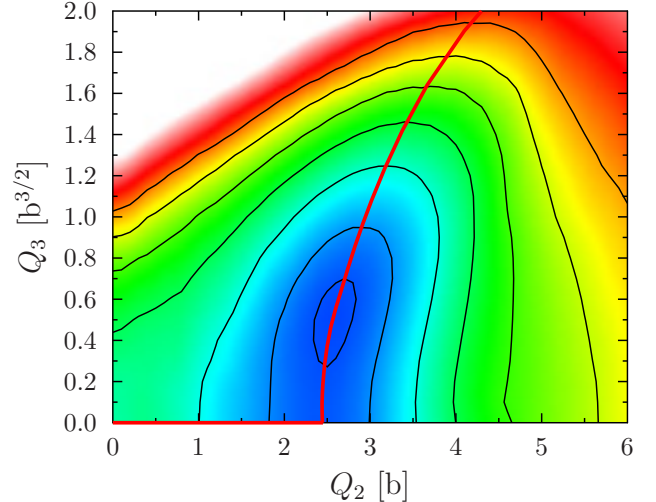


FIG. 3. Potential energy surface of the ^{142}Xe in the quadrupole (Q_{20}) - octupole (Q_{30}) plane calculated with the CHF+BCS method. The iso-energy contour line are separated by an energy of 2 MeV. The red thick line represents the minimum energy at a given quadrupole deformation.

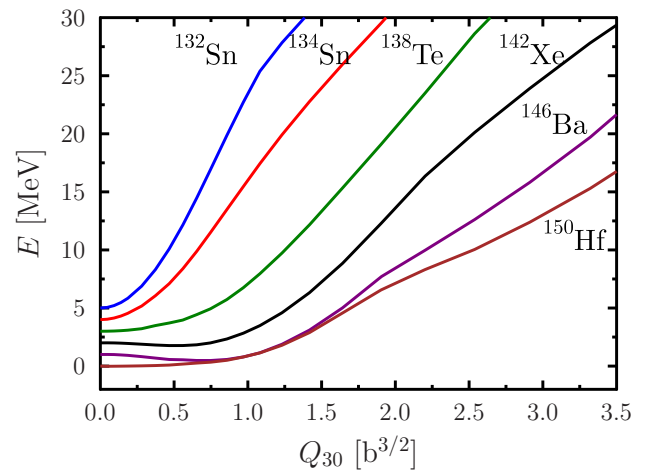


FIG. 4. CHF+BCS calculations of octupole energy for several isotopes produced in fission of actinides. The reference energy is shifted up by 1 MeV steps for each curve to improve clarity of the figure.

The octupole deformation energy has been calculated (without constraint on the quadrupole moment) and shown in Fig. 4 for some possible fission fragments of actinides. While ^{142}Xe and ^{146}Ba are predicted with an octupole minimum, this octupole softness disappears for tin (Sn, $Z = 50$) magic nuclei. Our calculations show that indeed, tin fragments produced in ^{258}Fm fission have

octupole moments 2 to 3 times smaller at scission than those with $Z \approx 55$. Fragments produced with $Z \approx 52$ also exhibits a significant octupole deformation, though not as strong as $Z \approx 55$ fragments, in agreement with the observation that ^{138}Te is less soft than ^{142}Xe and ^{146}Ba . For instance, the octupole deformation parameter is $\beta_3 \simeq 0.065$ (respectively 0.097) in a $\langle Z \rangle \simeq 52.6$ (55.37) fission fragment of ^{246}Cm at scission. The case of the doubly magic ^{132}Sn spherical nucleus is interesting. On the one side, its production as a fission fragment is expected to be favoured because of its extra-binding energy originating from spherical shell effects. On the other side, it is very stiff to octupole deformations and its production as a fission fragment is hindered (by comparison with softer nuclei) as it does not benefit from strong couplings to octupole deformation.

The background color of Fig. 2 shows the curvature of the octupole deformation energy $\alpha = \lim_{Q_{30} \rightarrow 0} \frac{E}{Q_{30}^2}$ of the nuclei near their quadrupole deformed minimum energy at $Q_{30} = 0$ (corresponding to the curvature at origin in Fig. 4). The formation of octupole soft (small or negative values of α) fission fragments like ^{140}Xe is clearly favoured. The fact that fragments with $\langle Z \rangle \geq 56$ are not produced in the calculations (except for ^{258}Fm) can be interpreted by the larger energy cost to form more asymmetric fragments.

The origin of the octupole softness can be understood from the deformed shell structure of the nuclei. CHF+BCS neutron and proton single-particle energies in ^{142}Xe are plotted in Fig. 5, following the path of minimum energy for given quadrupole deformations (solid line in Fig. 3). We observe a closure of the $Z = 50$ ($N = 82$) spherical gap and the opening of $Z = 52$ and 56 ($N = 84$ and 88) deformed shell gaps which survive for a large range of octupole deformations. The matching between the positions of the proton deformed gaps and of the St1 and St2 fission modes is striking. Another surprising finding is that the St1 mode is not driven by the $Z = 50$ spherical gap, but rather by a deformed shell closure, surviving to large octupole deformations, and thus favouring the formation of fission fragments thanks to octupole couplings. In fact, amongst all actinides studied experimentally, only ^{258}Fm is clearly dominated by $Z = 50$ spherical shell effects, producing two symmetric tin fragments (although it also exhibits an asymmetric mode with a heavy fragment around $Z \approx 55$). However, asymmetric fission dominates in ^{256}Fm and lighter fermium isotopes, confirming the weak influence of $Z = 50$ in the formation of fission fragments.

The total kinetic energy (TKE) of the final fragments is another important property of the fission modes, with St1 being associated with a larger TKE (typically ~ 10 MeV) than St2 [18, 56]. The TKE have been computed (see supplemental material [41]) from TDHF+BCS following the method introduced in Ref. [29]. As expected from the complexity of the many-body dynamics, the

results exhibit strong fluctuations (typically a variation of 15 – 20 MeV between the lowest and highest TKE for each nucleus). However, the average TKE is in very good agreement with available experimental data [18, 57, 58]. In addition, a clear pattern is found, with 10 – 15 MeV less for heavy fragments with $Z \approx 54 – 56$ than with $Z \approx 52$, again in excellent agreement with experimental observation [18]. The lower TKE with $Z \approx 54 – 56$ is interpreted as an effect of the larger deformation of the fragments at scission. The comparison between symmetric and asymmetric modes will be the subject of a future work. However, for consistency, we have calculated the TKE of a ^{234}U symmetric fission mode and obtained a value of ~ 151 MeV. As expected from systematics [18], this TKE is smaller than the asymmetric fission TKE (156 – 176 MeV) [41].

It would be very useful to develop techniques to study the excitation energy and neutron evaporation of the fragments from TDHF+BCS, including well beyond scission, in order to investigate the well known “saw-tooth” characteristic of the evolution of the neutron multiplicity as a function of fragment mass number [59]. Another interesting extension of this work will be the study of fission in the neutron deficient mercury ($Z = 80$) region. The recent observation of asymmetric fission in $^{180,182}\text{Hg}$ [60, 61], which came as a surprise, could indeed be influenced by the expected octupole softness in the $Z \approx 34$ region [53].

B. Jurado, A. Chatillon and F. Farget are thanked for useful discussions at the early stage of this work. We also thank D. J. Hinde for his continuous support to this project. This work has been supported by the Australian Research Council under Grant No. DP160101254. The calculations have been performed in part at the NCI National Facility in Canberra, Australia, which is supported by the Australian Commonwealth Government.

* scamps@nucl.ph.tsukuba.ac.jp

† cedric.simenel@anu.edu.au

- [1] O. Hahn and F. Strassmann, *Naturwissenschaften* **27**, 11 (1939).
- [2] L. Meitner and O. R. Frisch, *Nature (London)* **143**, 239 (1939).
- [3] K.-H. Schmidt, S. Steinhäuser, C. Böckstiegel, A. Grawe, A. Heinz, A. R. Junghans, J. Benlliure, H.-G. Clerc, M. de Jong, J. Müller, M. Pfützner, and B. Voss, *Nucl. Phys. A* **665**, 221 (2000).
- [4] J.-F. Martin, J. Taieb, A. Chatillon, G. Blier, G. Boutoux, A. Ebran, T. Gobinet, L. Grente, B. Laurent, E. Pellereau, H. Ivarez Pol, L. Audouin, T. Aumann, Y. Ayyad, J. Benlliure, E. Casarejos, D. Cortina Gil, M. Caamao, F. Farget, and H. Weick, *Eur. Phys. J. A* **51** (2015).
- [5] C. Rodríguez-Tajes, F. Farget, X. Derkx, M. Caamano, O. Delaune, K.-H. Schmidt, E. Clément, A. Dijon,

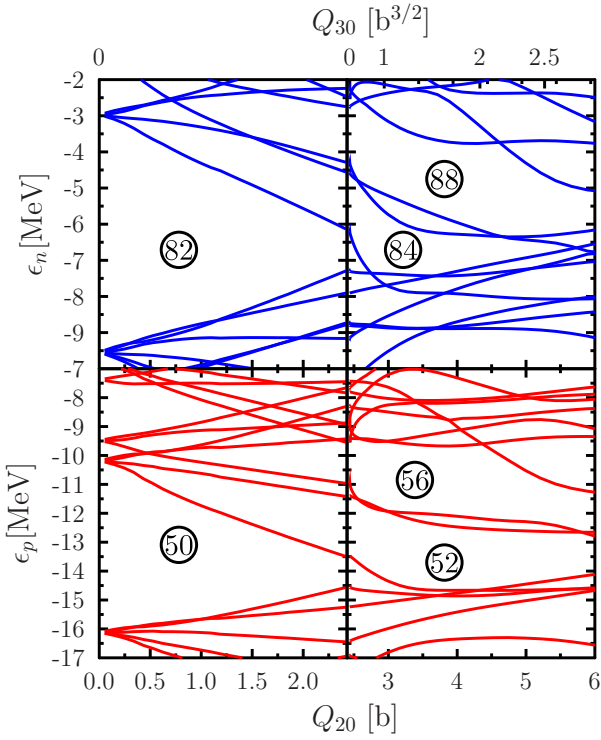


FIG. 5. Neutron (top) and proton (bottom) single-particle energies as a function of the quadrupole (lower scale) and octupole (upper scale) moments following the path of the solid line in Fig. 3.

A. Heinz, T. Roger, L. Audouin, J. Benlliure, E. Casarejos, D. Cortina, D. Doré, B. Fernández-Domínguez, B. Jacquot, B. Jurado, A. Navin, C. Paradela, D. Ramos, P. Romain, M. D. Salsac, and C. Schmitt, Phys. Rev. C **89**, 024614 (2014).

[6] I. V. Pokrovsky, M. G. Itkis, J. M. Itkis, N. A. Kondratiev, E. M. Kozulin, E. V. Prokhorova, V. S. Salamatin, V. V. Pashkevich, S. I. Mulgin, A. Y. Rusanov, S. V. Zhdanov, G. G. Chubarian, B. J. Hurst, R. P. Schmitt, C. Agodi, G. Bellia, L. Calabretta, K. Lukashin, C. Maiolino, A. Kelic, G. Rudolf, L. Stuttge, and F. Hanappe, Phys. Rev. C **62**, 014615 (2000).

[7] J. Khuyagbaatar, D. J. Hinde, I. P. Carter, M. Dasgupta, C. E. Düllmann, M. Evers, D. H. Luong, R. du Rietz, A. Wakhle, E. Williams, and A. Yakushev, Phys. Rev. C **91**, 054608 (2015).

[8] R. Léguillon, K. Nishio, K. Hirose, H. Makii, I. Nishinaka, R. Orlandi, K. Tsukada, J. Smallcombe, S. Chiba, Y. Aritomo, T. Ohtsuki, R. Tatsuzawa, N. Takaki, N. Tamura, S. Goto, I. Tsekhanovich, C. Petrache, and A. Andreyev, Phys. Lett. B **761**, 125 (2016).

[9] J. L. Rodríguez-Sánchez, J. Benlliure, J. Taïeb, H. Alvarez-Pol, L. Audouin, Y. Ayyad, G. Bélier, G. Boutoux, E. Casarejos, A. Chatillon, D. Cortina-Gil, T. Gorbinet, A. Heinz, A. Kelić Heil, B. Laurent, J.-F. Martin, C. Paradela, E. Pellereau, B. Pietras, D. Ramos, C. Rodríguez-Tajes, D. M. Rossi, H. Simon, J. Vargas, and B. Voss, Phys. Rev. C **94**, 061601 (2016).

[10] A. Göök, C. Eckardt, J. Enders, M. Freudenberger, A. Oberstedt, and S. Oberstedt, Phys. Rev. C **96**, 044301 (2017).

[11] E. Pellereau, J. Taïeb, A. Chatillon, H. Alvarez-Pol, L. Audouin, Y. Ayyad, G. Bélier, J. Benlliure, G. Boutoux, M. Caamaño, E. Casarejos, D. Cortina-Gil, A. Ebran, F. Farget, B. Fernández-Domínguez, T. Gorbinet, L. Grente, A. Heinz, H. Johansson, B. Jurado, A. Kelić Heil, N. Kurz, B. Laurent, J.-F. Martin, C. Nociforo, C. Paradela, S. Pietri, J. L. Rodríguez-Sánchez, K.-H. Schmidt, H. Simon, L. Tassan-Got, J. Vargas, B. Voss, and H. Weick, Phys. Rev. C **95**, 054603 (2017).

[12] K. Hirose, K. Nishio, S. Tanaka, R. Léguillon, H. Makii, I. Nishinaka, R. Orlandi, K. Tsukada, J. Smallcombe, M. J. Vermeulen, S. Chiba, Y. Aritomo, T. Ohtsuki, K. Nakano, S. Araki, Y. Watanabe, R. Tatsuzawa, N. Takaki, N. Tamura, S. Goto, I. Tsekhanovich, and A. N. Andreyev, Phys. Rev. Lett. **119**, 222501 (2017).

[13] J. Unik, J. Gindler, L. Glendenin, K. Flynn, A. Gorski, and R. Sjöblom, in *Proc. “Phys. and Chem. of Fission” IAEA Vienna*, Vol II (1974) p. 20.

[14] Nishio, Katsuhisa, Hirose, Kentaro, Mark, Vermeulen, Makii, Hiroyuki, Orlandi, Riccardo, Tsukada, Kazuaki, Asai, Masato, Toyoshima, Atsushi, Sato, Tetsuya K., Nagame, Yuichiro, Chiba, Satoshi, Aritomo, Yoshihiro, Tanaka, Shouya, Ohtsuki, Tsutomu, Tsekhanovich, Igor, Petrache, Costel M., and Andreyev, Andrei, EPJ Web Conf. **163**, 00041 (2017).

[15] U. Brosa, S. Grossmann, and A. Müller, Phys. Rep. **197**, 167 (1990).

[16] B. D. Wilkins, E. P. Steinberg, and R. R. Chasman, Phys. Rev. C **14**, 1832 (1976).

[17] M. Itkis, V. Okolovich, A. Rusanov, and G. Smirenkin, Sov. J. Part. Nucl. **19**, 301 (1988).

[18] C. Böckstiegel, S. Steinhäuser, K.-H. Schmidt, H.-G. Clerc, A. Grewe, A. Heinz, M. de Jong, A. Junghans, J. Müller, and B. Voss, Nucl. Phys. A **802**, 12 (2008).

[19] K.-H. Schmidt, B. Jurado, C. Amouroux, and C. Schmitt, Nuclear Data Sheets **131**, 107 (2016), special Issue on Nuclear Reaction Data.

[20] H. Goutte, J. F. Berger, P. Casoli, and D. Gogny, Phys. Rev. C **71**, 024316 (2005).

[21] W. Younes and D. Gogny, *Fragment yields calculated in a time-dependent microscopic theory of fission*, Tech. Rep. (Lawrence Livermore National Laboratory, Livermore, CA, 2012) technical Report LLNL-TR-586678.

[22] J. Sadhukhan, W. Nazarewicz, and N. Schunck, Phys. Rev. C **93**, 011304 (2016).

[23] J. Sadhukhan, C. Zhang, W. Nazarewicz, and N. Schunck, Phys. Rev. C **96**, 061301 (2017).

[24] A. Zdeb, A. Dobrowolski, and M. Warda, Phys. Rev. C **95**, 054608 (2017).

[25] N. Schunck and L. M. Robledo, Rep. Prog. Phys. **79**, 116301 (2016).

[26] K.-H. Schmidt and B. Jurado, HAL:in2p3-01314814 (2016).

[27] A. Wakhle, C. Simenel, D. J. Hinde, M. Dasgupta, M. Evers, D. H. Luong, R. du Rietz, and E. Williams, Phys. Rev. Lett. **113**, 182502 (2014).

[28] M. Morjean, D. J. Hinde, C. Simenel, D. Y. Jeung, M. Airiau, K. J. Cook, M. Dasgupta, A. Drouart, D. Jacquet, S. Kalkal, C. S. Palshetkar, E. Prasad, D. Rafferty, E. C. Simpson, L. Tassan-Got, K. Vo-Phuoc, and E. Williams, Phys. Rev. Lett. **119**, 222502 (2017).

[29] C. Simenel and A. S. Umar, Phys. Rev. C **89**, 031601(R)

(2014).

[30] P. M. Goddard, P. D. Stevenson, and A. Rios, *Phys. Rev. C* **92**, 054610 (2015).

[31] P. M. Goddard, P. D. Stevenson, and A. Rios, *Phys. Rev. C* **93**, 014620 (2016).

[32] G. Scamps, C. Simenel, and D. Lacroix, *Phys. Rev. C* **92**, 011602(R) (2015).

[33] Y. Tanimura, D. Lacroix, and G. Scamps, *Phys. Rev. C* **92**, 034601 (2015).

[34] Y. Tanimura, D. Lacroix, and S. Ayik, *Phys. Rev. Lett.* **118**, 152501 (2017).

[35] A. Bulgac, P. Magierski, K. J. Roche, and I. Stetcu, *Phys. Rev. Lett.* **116**, 122504 (2016).

[36] C. L. Zhang, B. Schuetrumpf, and W. Nazarewicz, *Phys. Rev. C* **94**, 064323 (2016).

[37] G. Scamps and D. Lacroix, *Phys. Rev. C* **87**, 014605 (2013).

[38] Ka-Hae Kim, Takaharu Otsuka, and Paul Bonche, *J. Phys. G* **23**, 1267 (1997).

[39] T. H. R. Skyrme, *Phil. Mag.* **1**, 1043 (1956).

[40] P. Bonche, H. Flocard, and P. H. Heenen, *Comput. Phys. Commun.* **171**, 49 (2005).

[41] See Supplemental Material at [URL will be inserted by the editor] for an extended discussion of the calculations presented in this work.

[42] A. D. Becke and K. E. Edgecombe, *J. Chem. Phys.* **92**, 5397 (1990), <https://doi.org/10.1063/1.458517>.

[43] P. Jerabek, B. Schuetrumpf, P. Schwerdtfeger, and W. Nazarewicz, *Phys. Rev. Lett.* **120**, 053001 (2018).

[44] B. Schuetrumpf and W. Nazarewicz, *Phys. Rev. C* **96**, 064608 (2017).

[45] P. Möller, D. G. Madland, A. J. Sierk, and A. Iwamoto, *Nature* **409**, 785 (2001).

[46] N. Carjan, F. Ivanyuk, and Y. Oganessian, *Nucl. Phys. A* **968**, 453 (2017).

[47] C. R. Morton, M. Dasgupta, D. J. Hinde, J. R. Leigh, R. C. Lemmon, J. P. Lestone, J. C. Mein, J. O. Newton, H. Timmers, N. Rowley, and A. T. Kruppa, *Phys. Rev. Lett.* **72**, 4074 (1994).

[48] A. M. Stefanini, B. R. Behera, S. Beghini, L. Corradi, E. Fioretto, A. Gadea, G. Montagnoli, N. Rowley, F. Scarlassara, S. Szilner, and M. Trotta, *Phys. Rev. C* **76**, 014610 (2007).

[49] N. Rowley and K. Hagino, *Nucl. Phys. A* **834**, 110c (2010).

[50] C. Simenel, M. Dasgupta, D. J. Hinde, and E. Williams, *Phys. Rev. C* **88**, 064604 (2013).

[51] D. Bourgin, C. Simenel, S. Courtin, and F. Haas, *Phys. Rev. C* **93**, 034604 (2016).

[52] L. P. Gaffney, P. A. Butler, M. Scheck, A. B. Hayes, F. Wenander, M. Albers, B. Bastin, C. Bauer, A. Blazhev, S. Bönig, N. Bree, J. Cederkäll, T. Chupp, D. Cline, T. E. Cocolios, T. Davinson, H. De Witte, J. Diriken, T. Grahn, A. Herzan, M. Huyse, D. G. Jenkins, D. T. Joss, N. Kesteloot, J. Konki, M. Kowalczyk, T. Kröll, E. Kwan, R. Lutter, K. Moschner, P. Napiorkowski, J. Pakarinen, M. Pfeiffer, D. Radeck, P. Reiter, K. Reynders, S. V. Rigby, L. M. Robledo, M. Rudigier, S. Sambi, M. Seidlitz, B. Siebeck, T. Stora, P. Thoelle, P. Van Duppen, M. J. Vermeulen, M. von Schmid, D. Voulot, N. Warr, K. Wimmer, K. Wrzosek-Lipska, C. Y. Wu, and M. Zielinska, *Nature* **497**, 199 EP (2013).

[53] P. A. Butler, *J. Phys. G* **43**, 073002 (2016).

[54] B. Bucher, S. Zhu, C. Y. Wu, R. V. F. Janssens, D. Cline, A. B. Hayes, M. Albers, A. D. Ayangeakaa, P. A. Butler, C. M. Campbell, M. P. Carpenter, C. J. Chiara, J. A. Clark, H. L. Crawford, M. Cromaz, H. M. David, C. Dickerson, E. T. Gregor, J. Harker, C. R. Hoffman, B. P. Kay, F. G. Kondev, A. Korichi, T. Lauritsen, A. O. Macchivelli, R. C. Pardo, A. Richard, M. A. Riley, G. Savard, M. Scheck, D. Seweryniak, M. K. Smith, R. Vondrasek, and A. Wiens, *Phys. Rev. Lett.* **116**, 112503 (2016).

[55] S. Ebata and T. Nakatsukasa, *Physica Scripta* **92**, 064005 (2017).

[56] H. H. Knitter, F. J. Hambach, and C. Budtz-Jorgensen, *Z. Naturf.* **42a**, 786 (1987).

[57] C. Wagemans, E. Allaert, A. Deruytter, R. Barthélémy, and P. Schillebeeckx, *Phys. Rev. C* **30**, 218 (1984).

[58] M. Caamaño, F. Farget, O. Delaune, K.-H. Schmidt, C. Schmitt, L. Audouin, C.-O. Bacri, J. Benlliure, E. Casarejos, X. Derkx, B. Fernández-Domínguez, L. Gaudefroy, C. Golabek, B. Jurado, A. Lemasson, D. Ramos, C. Rodríguez-Tajes, T. Roger, and A. Shrivastava, *Phys. Rev. C* **92**, 034606 (2015).

[59] J. S. Fraser and J. C. D. Milton, *Phys. Rev.* **93**, 818 (1954).

[60] A. N. Andreyev, J. Elseviers, M. Huyse, P. Van Duppen, S. Antalic, A. Barzakh, N. Bree, T. E. Cocolios, V. F. Comas, J. Diriken, D. Fedorov, V. Fedossev, S. Franchoo, J. A. Heredia, O. Ivanov, U. Köster, B. A. Marsh, K. Nishio, R. D. Page, N. Patronis, M. Seliverstov, I. Tsekhanovich, P. Van den Bergh, J. Van De Walle, M. Venhart, S. Vermote, M. Veselsky, C. Wagemans, T. Ichikawa, A. Iwamoto, P. Möller, and A. J. Sierk, *Phys. Rev. Lett.* **105**, 252502 (2010).

[61] E. Prasad, D. J. Hinde, K. Ramachandran, E. Williams, M. Dasgupta, I. P. Carter, K. J. Cook, D. Y. Jeung, D. H. Luong, S. McNeil, C. S. Palshetkar, D. C. Raferty, C. Simenel, A. Wakhle, J. Khuyagbaatar, C. E. Düllmann, B. Lommel, and B. Kindler, *Phys. Rev. C* **91**, 064605 (2015).